Experimental and modelling study of water condensation and evaporation at the surface of fruits during cold chain breaks

Gurvan Lequentrec, Nattawut Chaomuang, Patrick Sambou, Graciela Alvarez, D. Flick, Steven Duret

DOI: 10.18462/iir.icr.2023.0515

Experimental and modelling study of water condensation and evaporation at the surface of fruits during cold chain breaks

Gurvan LEQUENTREC [(a)], Nattawut CHAOMUANG[(b)], Patrick SAMBOU[(a)], Graciela ALVAREZ[(a)], Denis FLICK[(c)] Steven DURET*[(a)]

[(a)] Université Paris-Saclay, INRAE, FRISE, 92761, Antony, France
[(b)] King Mongkut's Institute of Technology Ladkrabang, Thailand
[(c)]Université Paris-Saclay, INRAE, AgroParisTech, UMR SayFood, 91300 Massy, France

*Corresponding author: steven.duret@inrae.fr

ABSTRACT

In the fruits and vegetables cold chain, condensation may occur due to temperature fluctuations in the equipment or when cold products are submitted, to ambient air during the transfer from one link to another. Free water at the product surface may remain for a long period as the humidity in the equipment is usually high (>80%), limiting thus water evaporation. The presence of liquid water at the product surface is generally not suitable as it promotes spoilage micro-organisms. On the other hand, condensed water and high humidity reduces product transpiration thus preventing weight loss.
This study presents the evolution of the quantity of condensed water on fruit surface during cold chain breaks and during the following storage at low temperature and high humidity. A model predicting product temperature, air temperature and humidity and the amount of condensed water at the product surface was developed and validated with experimental measurements.

Keywords: Condensation, cold chain breaks, heat transfer, mass transfer, quality

1. INTRODUCTION

In the post-harvest chain of fruit and vegetables, temperature is the main factor influencing the evolution of the organoleptic qualities of the food products. For this reason, temperature control through the cold chain is of major importance to reduce food waste and provide consumers with products with high qualities. However, humidity is usually not controlled in the cold chain and relatively high (>70%). This high humidity, associated with temperature fluctuations may cause condensation on the surface (Ben-Yehoshua et al. 2005). Condensation may also occurs when cold products are submitted during transfer from one step to another, even briefly, at ambient conditions and medium humidity (e.g. 25°C, 50%HR).
The presence of liquid water at the surface of the product is generally not suitable for product quality, especially if it remains for a long period as it promotes micro-organisms (Wang et al. 2015). The development of molds in the fruits and vegetable post-harvest chain remains an issue. It is estimated that half of the fruits and vegetables harvested in the tropics are lost due to fungal spoilage (Pitt and Hocking 2009). On the other hand, condensed water at the product surface and high humidity reduces product transpiration and thus prevent weight loss and shrinkage (Linke et al. 2021).
Condensation occurs when surface temperature is below air dew temperature. Because of the complexity of the airflow due to the shape of the products, the nature of the packaging and the variety of pallet arrange (Smale et al. 2006), condensation and evaporation can occur at the same time in a pallet and even on a single product. While many experimental and numerical studies were conducted on weight loss according to temperature and humidity conditions during storage (Duret et al. 2014, Kim et al. 2020), few studies considered condensation and evaporation in the cold chain. Laguerre et al. (2010) studied the simultaneous water evaporation and condensation in a refrigerator loaded with wet products. Gottschalk et al. (2007) conducted and experimental and numerical study on the condensation and evaporation of water on a single product surface during rewarming in ambient air. The authors determined the amount of condensed water as well as the total dwell time according to environmental conditions.

The objective of the present paper is to study the evolution of the quantity of water on horticultural fruit surface during cold chain break event. Two different configurations are studied, a single product whose temperature is homogeneous (Biot number <0.1, aluminum sphere) and a single product whose temperature is heterogeneous (Biot number > 0.1, citrus fruit). Simplified models are proposed to predict heat and mass transfer phenomenon.

2. MATERIAL AND METHODS

2.1. Experimental set-up

Fig. 1 presents the experimental set-up with dimensions 1.2x0.4x0.2 m (LxWxH) and made of polystyrene material. This whole set-up was located in a cold room set at 4°C in which humidity was measured but not controlled (~80-90 RH%). A fan at the exit of the experimental set-up was controlled with a potentiometer to set air velocity (0.33 $m.s^{-1}$). The system included two entrance, one cold entrance using the ambient air of the cold room and one warm and humid air entrance. Air temperature and vapor rate (and hence humidity) were controlled using electrical resistance whose power was controlled manually. A switching shutter allowed the instantaneous switch between the cold and hot entrances. The objective was to apply a rapid transition to create, for example, loading/unloading conditions in a truck.
Experiments were first conducted on a single aluminum sphere (diameter D = 0.07 m, conductivity λ = 237 $W.m^{-1}.°C^{-1}$, Cp = 897 $J.kg^{-1}.K^{-1}$, emissivity ε = 0.12, Biot number <0.1). Then experiments were conducted on a single orange fruit (D=0.073 m, λ=0.43 W.m-^{1}.°C^{-1}, Cp = 4200 $J.kg^{-1}.K^{-1}$, ρ=959 $kg.m^{-3}$ Biot number > 0.1).

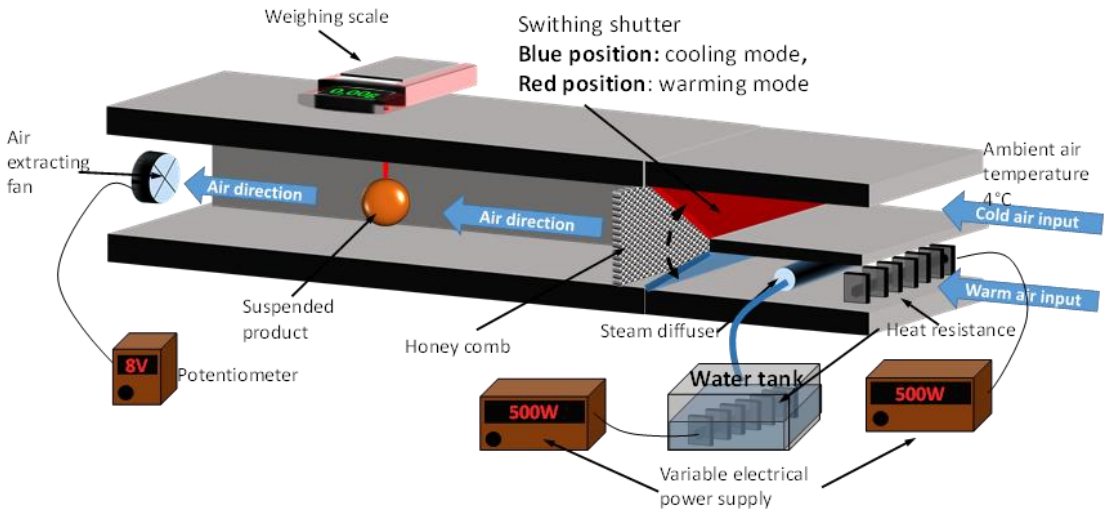

Figure 1: Experimental set-up

2.2 Temperature, humidity, air velocity, weight measurements and condensation detection

T-type thermocouples (1mm diameter, precision ± 0.2 °C) calibrated at 5 different temperatures (0°C, 10°C, 20°C, 30°C and 40°C) were used. These thermocouples were used to measure temperatures at the center of the product, at the surface, in the air and on the experimental wall surface. Hygrometer Vaisala HMP110 (range 0/100 % HR; -40/+80 °C, accuracy 1.5%HR) were used to measure the relative humidity of the air at different position in the experiment set-up. Air velocity measurement was measurement using hot wire anemometer (TESTO 435-4, range 0 - 20 $m.s^{-1}$ and calibrated accuracy assured by the supplier of 5% of the read value or ±0.03 $m.s^{-1}$). Ohaus Explorer 10200 g/0.01g were used to continuously measure water quantity at the surface of the products. Finally, on the orange fruit only, wetness detectors were placed at the front and the rear of the product. The device consists measuring electrical resistivity between two slates of copper placed on the surface (Linke et al. 2021).

2.2.1 Heat transfer coefficient measurement

The convective heat transfer coefficient was measured using an aluminum sphere cooled down from 20°C to 4°C. The convective heat transfer coefficient h was calculated from the slope of the curve $\left(= - \frac{hA}{mC} \right)$ describing the evolution of $\ln(T^*) = \ln\left(\frac{T - T_{eq}}{T_0 - T_{eq}} \right)$ in function of time. The convective heat transfer coefficient was found to be 9.0 $W.m^{-2}.°C^{-1}$. This value is in agreement with the value calculated from Kramers correlation ($h_{Kramers}$ = 8.9 $W.m^{-2}.°C^{-1}$) (Kramers 1946).

$$Nu = 2 + 1.3 \cdot Pr^{0.15} + 0.66 \cdot Pr^{0.31} \cdot Re^{0.5} \quad \text{Eq. (1)}$$

$$h_{Kramers} = \frac{Nu \cdot \lambda}{D} \quad \text{Eq. (2)}$$

This value also corresponds to measured convective heat transfer coefficient measured for food products in pallets convective heat transfer coefficient (min =2 $W.m^{-2}.°C^{-1}$ and max = 20 $W.m^{-2}.°C^{-1}$)(Duret et al. 2014, Laguerre et al. 2014). Heat transfer due to natural convection was neglected ($Ri \sim 0.3$, at the initial conditions, T_p = 20°C and T_{air} = 5°C).

2.3 Studied conditions.

For all experiments, initial product temperature is at 5°C, products are submitted to an air at 25°C during 30 min and then cooled back at 4°C. A second condition consisted in warming up the products until equilibrium. Two hygrometry were tested (~50% and ~70%) for an air velocity of 0.3 $m.s^{-1}$.

2.4. Modelling heat and mass transfer

First, two simple models for the single product were developed to predict heat and mass transfer between the sphere and ambient air.
For the aluminium sphere (Bi<<0.1), the temperature is considered homogeneous, hence, the temperature can be predicted with eq.1 :

$$m_p \cdot Cp_p \cdot \frac{\partial T_p}{\partial t} = h \cdot S \cdot \left(T_a - T_{sphere}\right) + L_v \cdot \dot{m} + \varepsilon \cdot \sigma \cdot S \cdot \beta_w \cdot \left(T_{wall}^4 - T_{sphere}^4\right) \quad \text{Eq. (3)}$$

$$\dot{m} = k \cdot S \cdot \beta_w \cdot \left(C_{sat(T_{sphere})} - C_{wa}\right) \quad \text{Eq. (4)}$$

β_w represents the ratio between the wetted surface and the sphere surface. During the condensation phase, β_w = 1 as the condensation was assumed uniform on the surface. For the evaporation phase, β_w = 1 if the mass of water m_w was superior to threshold value m_T of 0.3 g (m_T is a threshold value under which the wetted surface starts to decrease during the evaporation phase, determined experimentally – results not shown). For m_w< 0.3g:

$$\beta_w = \frac{m_w}{m_c} \quad \text{Eq. (5)}$$

The Lewis analogy (*Le*) was used to estimate the mass transfer coefficient *k*.

$$k = \frac{h}{\rho_a \cdot Cp_a \cdot Le^{2/3}} \text{ with } Le = \frac{a_{diff}}{D_w} \approx 0.85 \quad \text{Eq. (6)}$$

a_{diff} is the thermal diffusivity of water vapor = $18.6 \cdot 10^{-6}$ $m^2.s^{-1}$ at 0°C,
D_w is the mass diffusivity of water vapor in air = $21.8 \cdot 10^{-6}$ $m^2.s^{-1}$ at 0°C.

For the orange fruit product, as Bi>0.1 the homogeneity of the product temperature cannot be considered, the heat transfer was modelled using:

$$\frac{1}{\alpha}\cdot\frac{\partial T}{\partial t}=\frac{1}{r^2}\cdot\frac{\partial T}{\partial r}\left(r^2\cdot\frac{\partial T}{\partial r}\right) \qquad \text{Eq. (7)}$$

At the core and at the surface, symmetry and Newmann boundary conditions were considered, respectively.

$$\left.\frac{\partial T}{\partial r}\right|_{r=0}=0 \qquad \text{Eq. (8)}$$

$$-\lambda\left.\frac{\partial T}{\partial r}\right|_{r=R}=h\cdot(T_a-T_s)+L_v\cdot k\cdot\beta_w\cdot\left(C_{sat(T_{sphere})}-C_{wa}\right)+\varepsilon\cdot\sigma\cdot\left(T_{wall}^4-T_s^4\right) \qquad \text{Eq. (9)}$$

Equations were solved using FTCS (Forward Time Centered Space) method (Thibault et al. 1987). Because of its non-linearity, an iterative process was used to solve Eq. (9).

3. RESULTS & DISCUSSION

Fig. 2 presents results obtained with the aluminum sphere, initially cold (5°C) and submitted for 30 min to a warm air (~25°C ,60 RH%). Both experimental and predicted values of temperature and mass of water are presented. During the first 20 minutes, the saturated vapor concentration at the surface temperature is lower than the vapor concentration in the air which induces condensation. The mass of water at the sphere surface rapidly increases. After 20 min, as the sphere temperature increases and reach the dew point temperature ($C_{air} \sim C_{sat}(T_s)$), the condensation rate decreases and the mass of water stabilizes. After 25 min, the vapor concentration at surface temperature is slightly higher than the vapor concentration in the air (Fig. 2C), starting then slowly the evaporation of the water at the product surface. After 30 min, the product is submitted to a cold air. As the vapor concentration is much lower in the air than the saturated vapor concentration at the product surface temperature, the evaporation of the water evaporation at the product surface is rapid. Hence, after 45 min, the water is completely evaporated. Model predictions for both sphere temperature and mass of water at the surface are in agreement with the measured value. Slight difference might be due to the evaluation of the convective heat transfer coefficient.

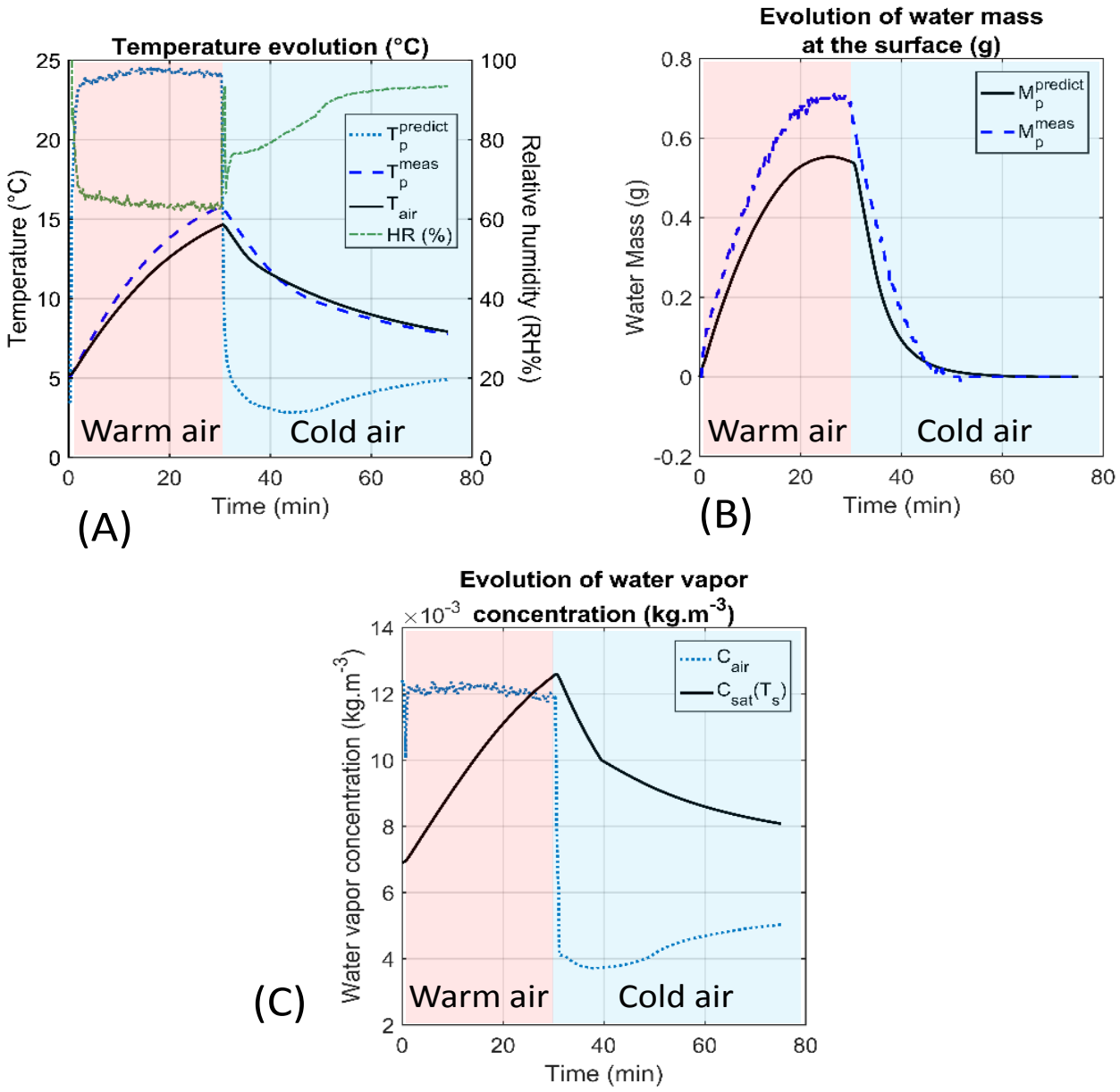

Figure 2: Evolution during successive warming and cooling, of the aluminum sphere temperature, air temperature and relative humidity (A), mass of water condensed on the surface (B), Evolution of water vapor concentration (C). Warming period (~25°C, 60 RH%) is represented by the red area, cold period (4°C, 80-90 RH%) is represented by the blue area.

Fig. 3 presents results obtained with the aluminum sphere, initially cold (4°C) and submitted continuously to a warm air (~24°C,60 RH%). Both experimental and predict values of temperature and mass of water are presented. During the first 20 minutes, as expected, results are very similar to Fig. 2 and the mass of water at the sphere surface rapidly increases due to condensation. After 20 min, as the sphere temperature increases and reach the dew point temperature, the condensation rate decreases and the mass of water stabilizes. After 25 min, the saturated vapor concentration at surface temperature is slightly higher than the vapor concentration in the air, starting then slowly the evaporation of the water at the product surface. Evaporation rate increases and water mass decreases rapidly as the product temperature increases. Finally, because the wetted area decreases, the evaporation rate starts decreasing after 45 min. All the water was evaporated after 80 min.

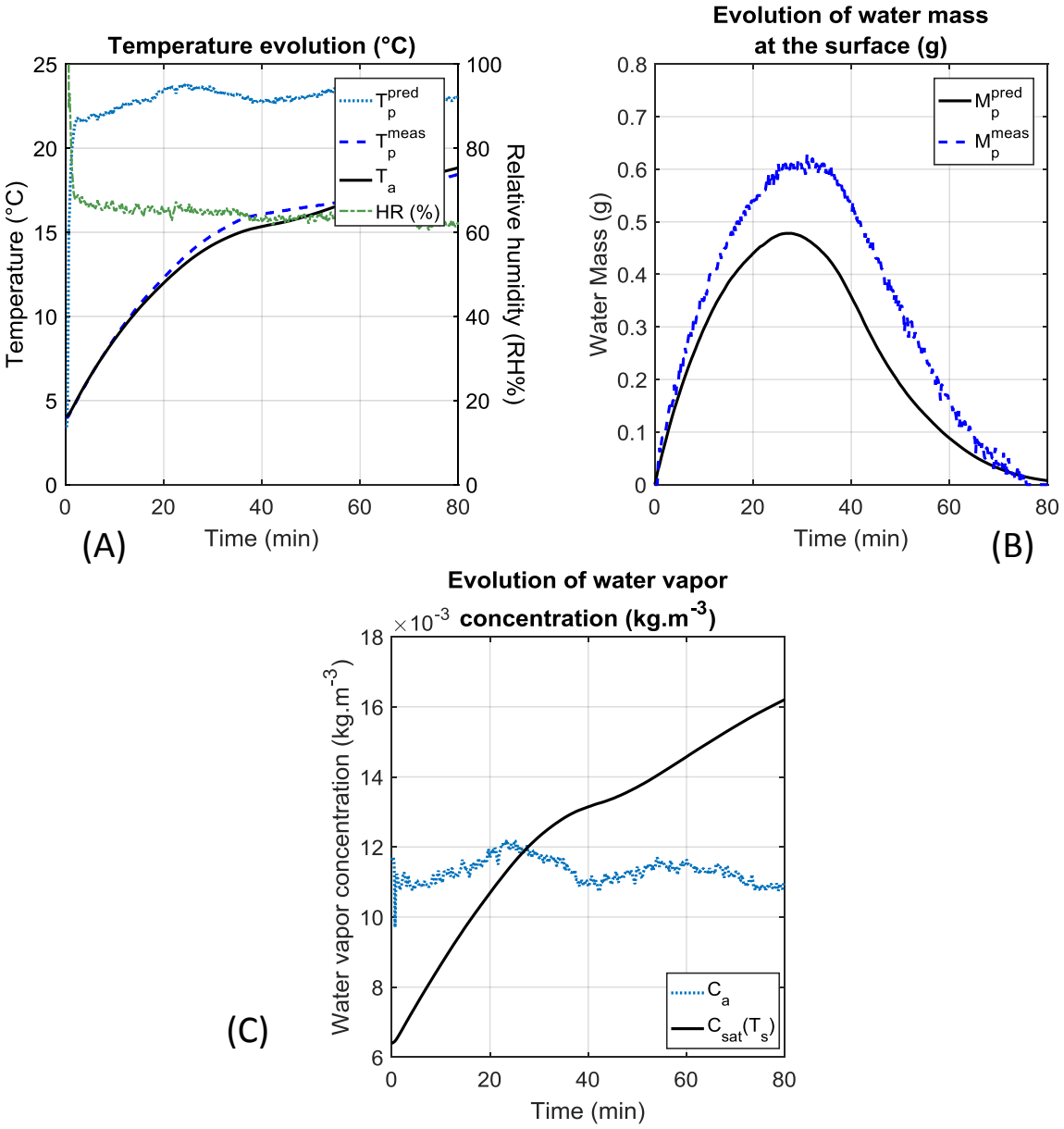

Figure 3: Evolution during warming from 4°C to 24°C of the aluminum sphere temperature, air temperature and relative humidity (60 RH%) (A), mass of water condensed on the surface (B), Evolution of water vapor concentration (C).

Fig. 4 presents results obtained with the orange fruit, initially cold (5°C) submitted continuously to a warm air (25°C, 60 RH%). Both experimental and predict values of temperature and mass of water are presented. The condensation occurs during the first 20 minutes before stabilizing until 30 minutes, when the product is placed under the cold air and evaporation take place rapidly. The measured value at the surface (front and rear of the product) are higher than the predict surface temperature, this is probably because surface temperature were measured using thermocouple taped on the surface, then the measured value is actually a mix between actual surface temperature and air temperature. However, surface temperature is still interesting to observe. Indeed, the surface temperature at the front increases faster than at the rear, meaning that the water is evaporating first at the front while still condensing at the rear. Hence, it is then expected that the water will remain longer at the rear than at the front. This observation is supported also by the wetness detectors (Fig. 4 D). The wetness detector at the front suggests that the water is evaporated at 30 min while at the rear, the water remains until 45 min, which also corresponds to the value of the water mass that indicates that the water is completely evaporated at 50 min (Fig. 4D). This aspect is important as for further studies in more complex geometries such as a pallet, the measurement of the water mass might be difficult. As an alternative, wetness detector seem to be a qualitative, but reliable information of the presence of water. This

aspect is particularly important as the input of microbial model for example to estimation spore germination is usually the wetness duration rather than the actual quantity of water.

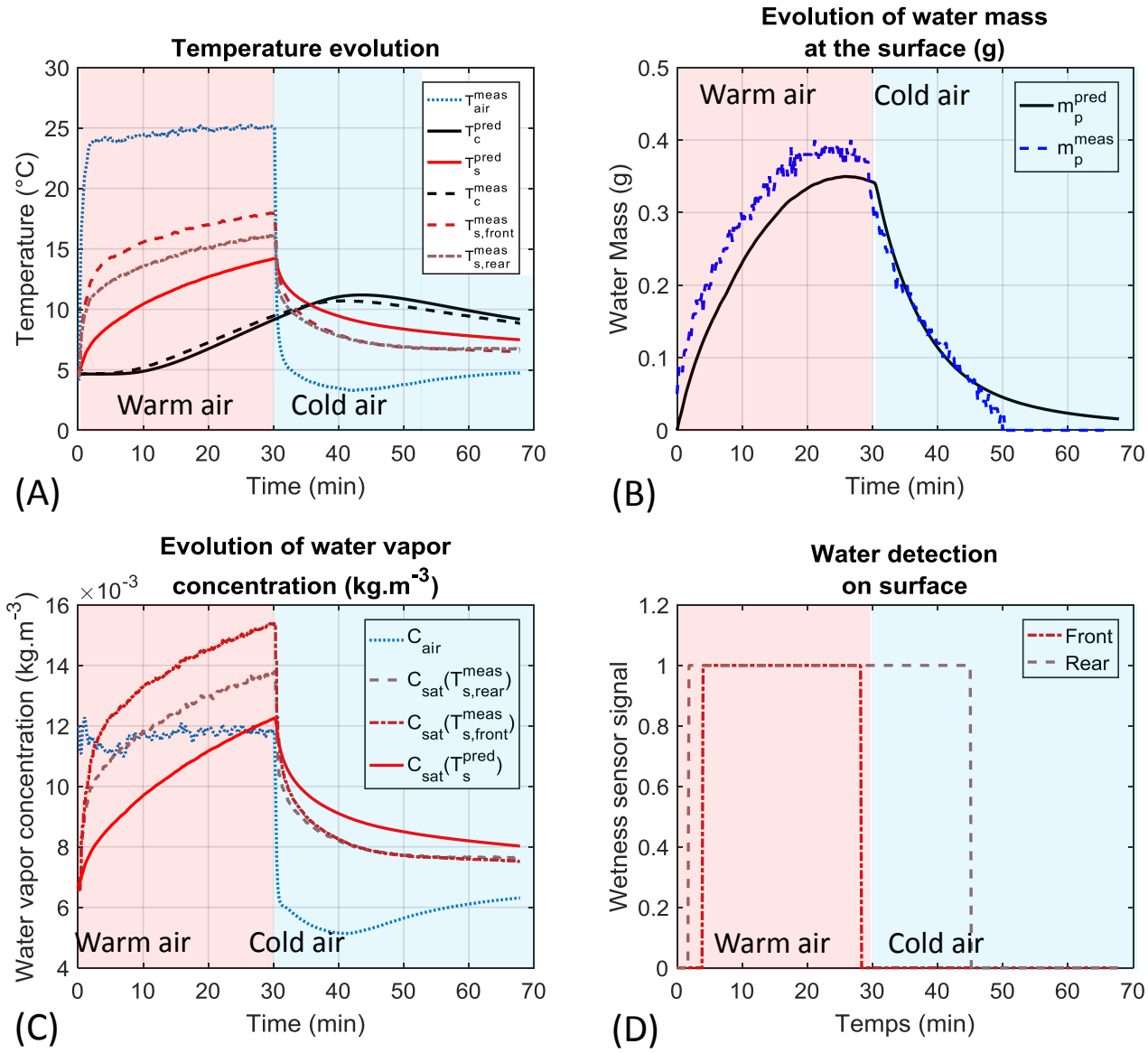

Figure 4: Evolution during successive warming and cooling, of the orange fruit temperature and air temperature (A), mass of water condensed on the surface (B), Evolution of water vapor concentration (C). Detection of water condensate at the product surface (D). Warming period (~25°C, 60 RH%) is represented by the red area, cold period (4°C, 80-90 RH%) is represented by the blue area.

4. CONCLUSIONS

A study of water condensation and evaporation at the surface of food products was conducted to simulate cold chain break, for example, during truck loading/unloading. Experiments were carried out on an aluminum sphere and on as orange fruit. For both cases, a model was developed to predict temperature and mass water evolution. Results show that condensation and evaporation on a single product are heterogeneous, leading on a single product to condensation and evaporation simultaneously. Wetness detectors were used, results show that the sensors were able to give a good approximation of the wetness duration in comparison to the actual measurement of the water mass, which will be useful for further studies in more complex geometry such as pallets.

ACKNOWLEDGEMENTS

The authors thank the INRAE TRANSFORM Department for the funding of this study.

NOMENCLATURE

C	vapor concentration ($kg.m^{-3}$)
Cp	thermal heat capacity ($J.kg^{-1}.°C^{-1}$)
D	diameter (m)
D_w	mass diffusivity of vapor in air ($m^2.s^{-1}$)
g	gravitational acceleration ($9.81\ m.s^{-1}$)
h	convective heat transfer coefficient ($W.m^{-2}.°C^{-1}$)
k	mass transfer coefficient ($m.s^{-1}$)
L_v	Latent heat of evaporation ($J.kg^{-1}$)
m	mass (kg)
S	surface (m^2)
t	time (s)
T	temperature (°C)

Greek letters

α	thermal diffusivity ($m^2.s^{-1}$)
ε	emissivity
λ	thermal conductivity ($W.m^{-1}.°C^{-1}$)
μ	dynamic viscosity (Pa.s)
ν	kinematic viscosity ($m^2.s^{-1}$)
ρ	density ($kg.m^{-3}$)
σ	Stefan-Boltzmann constant ($5.67 \cdot 10^{-8}\ W.m^{-2}.K^{-4}$)

Subscrits

0	initial value
a	air
c	core
eq	equilibrium
meas	measured
p	product
pred	predicted
s	surface
sat	saturation
w	water

REFERENCES

Ben-Yehoshua, S., R. M. Beaudry, S. Fishman, S. Jayanty and N. Mir, 2005. Modified atmosphere packaging and controlled atmosphere storage. Environmentally Friendly Technologies for Agricultural Produce Quality, 61-112.

Duret, S., H. M. Hoang, D. Flick and O. Laguerre, 2014. Experimental characterization of airflow, heat and mass transfer in a cold room filled with food products. International Journal of Refrigeration, 46,(17-25).

Gottschalk, K., M. Linke, C. Mészáros and I. Farkas, 2007. Modeling Condensation and Evaporation on Fruit Surface. Drying Technology, 25,(7-8), 1237-1242.

Kim, S.-H., C. Nishihara, F. Tanaka and F. Tanaka, 2020. Simulation of Temperature Profile and Moisture Loss of Fresh Cucumber Fruit and Visualization of Commercial Storage Duration. Food Science and Technology Research, 26,(4), 459-468.

Kramers, H., 1946. Heat transfer from spheres to flowing media. Physica, 12,(2), 61-80.

Laguerre, O., S. Benamara and D. Flick, 2010. Study of water evaporation and condensation in a domestic refrigerator loaded by wet product. Journal of Food Engineering, 97,(1), 118-126.

Laguerre, O., S. Duret, H. M. Hoang and D. Flick, 2014. Using simplified models of cold chain equipment to assess the influence of operating conditions and equipment design on cold chain performance. International Journal of Refrigeration, 47,120-133.

Linke, M., U. Praeger, P. V. Mahajan and M. Geyer, 2021. Water vapour condensation on the surface of bulky fruit: Some basics and a simple measurement method. Journal of Food Engineering, 307,110-661.

Pitt, J. I. and A. D. Hocking (2009). Fresh and Perishable Foods. Fungi and Food Spoilage. J. I. Pitt and A. D. Hocking. Boston, MA, Springer US: 383-400.

Smale, N. J., J. Moureh and G. Cortella, 2006. A review of numerical models of airflow in refrigerated food applications. International Journal of Refrigeration, 29,(6), 911-930.

Thibault, J., S. Bergeron and H. W. Bonin, 1987. On finite-difference solutions of the heat equation in spherical coordinates. Numerical Heat Transfer, 12,(4), 457-474.

Wang, B., B.-H. Li, X.-L. Dong, C.-X. Wang and Z.-F. Zhang, 2015. Effects of Temperature, Wetness Duration, and Moisture on the Conidial Germination, Infection, and Disease Incubation Period of Glomerella cingulata. Plant Disease, 99,(2), 249-256.